remote sensing

Article

Enhancement of Cloud-to-Ground Lightning Activity Caused by the Urban Effect: A Case Study in the Beijing Metropolitan Area

Yongping Wang [1], Gaopeng Lu [1], Tao Shi [1], Ming Ma [1], Baoyou Zhu [1], Dongxia Liu [2], Changzhi Peng [3] and Yu Wang [4,5,6,*]

1 School of Earth and Space Sciences, University of Science and Technology of China, Hefei 230000, China; wyp8966@mail.ustc.edu.cn (Y.W.); gplu@ustc.edu.cn (G.L.); shitao@mail.ustc.edu.cn (T.S.); mingma@ustc.edu.cn (M.M.); zhuby@ustc.edu.cn (B.Z.)
2 Institute of Atmospheric Physics, Chinese Academy of Sciences, Beijing 100000, China; liudx@mail.iap.ac.cn
3 School of Electrical Engineering and Automation, Wuhan University, Wuhan 430000, China; pengcz@whu.edu.cn
4 State Grid Electric Power Research Institute, Wuhan 430074, China
5 Wuhan NARI Co., Ltd. of State Grid Electric Power Research Institute, Wuhan 430074, China
6 Hubei Province Key Laboratory of Lightning Risk Prevention for Power Grids, Wuhan 430074, China
* Correspondence: wangyu16@sgepri.sgcc.com.cn

Abstract: To investigate the possible impact of urban development on lightning activity, an eight-year (2010–2017) cloud-to-ground (CG) lightning dataset provided by the National-Wide Lightning Detection Network in China was analyzed to characterize the CG lightning activity in the metropolitan area of Beijing. There is a high CG flash density area over the downtown of Beijing, but different from previous studies, the downwind area of Beijing is not significantly enhanced. Compared with the upwind area, the CG flash density in the downtown area was enhanced by about 50%. Negative CG flashes mainly occurred in the downtown and industrial area, while positive CG flashes were distributed evenly. The percentage of positive CG flashes with $I_{peak} \geq 75$ kA is more than six times that of the corresponding negative CG flashes in the Beijing area. The enhancement of lightning activity varies with season and time. About 98% of CG flashes occurred from May to September, and the peak of CG diurnal variation is from 1900 to 2100 local time. Based on the analysis of thunderstorm types in Beijing, it is considered that the abnormal lightning activity is mainly responsible for an enhancement of the discharge number in frontal systems rather than the increase of the number of local thunderstorms. In addition, there is a non-linear relationship between pollutant concentrations and CG flash number, which indicates that there are other critical factors affecting the production of lightning.

Keywords: cloud-to-ground lightning; megacity; urban effect; atmospheric pollutant

check for updates

Citation: Wang, Y.; Lu, G.; Shi, T.; Ma, M.; Zhu, B.; Liu, D.; Peng, C.; Wang, Y. Enhancement of Cloud-to-Ground Lightning Activity Caused by the Urban Effect: A Case Study in the Beijing Metropolitan Area. *Remote Sens.* **2021**, *13*, 1228. https://doi.org/10.3390/rs13071228

Academic Editor: Stefano Dietrich

Received: 13 February 2021
Accepted: 19 March 2021
Published: 24 March 2021

1. Introduction

Lightning activity is a common cause of power system failures, property damage, and weather-related deaths. Urbanization can influence the long-term behavior of regional cloud-to-ground (CG) lightning activity [1]. Since the 1980s, many studies have been conducted to investigate the impact of urban development on CG lightning activity in different geographical areas of the world [2–12]. Westcott [2] firstly proposed that the urban effect can enhance the lightning activity over and downwind of cities based on data from the National Lightning Detection Network in the United States. Steiger et al. [3] used data from the same lightning detection network and also reported that a significant enhancement of 45% in the CG flash density was observed over Houston, Texas compared to the nearby surrounding areas, and it was shown that the percentage of positive CG flashes exhibited a significant decrease (12%).

The urban effect is primarily a combination of the thermodynamic effect caused by the urban heat island (UHI) [13,14] and the increase of pollution concentration due to the plentiful anthropogenic activity [15,16]. The heat from downtown can modify local convective processes associated with thunderstorms [6], while pollutants in the boundary layer could uplift the concentration of cloud condensation nuclei and thus suppress the mean droplet size [5,17–19]. The enhancement impact of UHI on the lightning activity (thunderstorm lifetime and thunderstorm initiation) over cities has been relatively well understood [12], but there is no consensus on the role of pollutants on this enhancement. Since air pollution is influenced by different meteorological processes, it is not easy to infer the specific role of pollutants on the increase of CG lightning activity.

Based on CG lightning data from the lightning detection network deployed on the Iberian Peninsula that belongs to the Spanish Meteorological Institute, Soriano and de Pablo [4] analyzed the lightning activity in several small Spanish towns using the data of three years, and the results showed that the higher SO_2 (sulfur dioxide) concentration contributes to the increase in the number of CG flashes, while the PM_{10} contribution (i.e., particulate matter with aerodynamic diameter <10 μm) seems to be irrelevant. However, Naccarato et al. [6] showed that the PM_{10} concentration is positively correlated with the number of CG flashes over three large metropolitan areas in southeastern Brazil. It is likely because the air pollutants saturate the concentration of aerosol particles at a specific level, inhibiting the intensification of lightning activity [10,20]. Farias et al. [11] found that PM_{10} increases the lifetime of thunderstorms and the number of flashes per thunderstorm rather than the flash rate of thunderstorms, combined with pollutant data provided by the São Paulo environment agency. Kar et al. [8] and Kar and Liou [9] also indicated that the higher concentrations of PM_{10} and SO_2 contribute to the enhancement of CG lightning activity. Although considerable studies have been conducted on the influence of pollutants on the CG lightning activity, the present understanding is incomplete, and extensive studies are still needed.

With the rapid economic and social development, anthropogenic pollutant emissions and urban sprawl have had an increasing impact on lightning activity. With the increase of the world's population, the number of megacities is also growing rapidly. Most existing studies regarding the urban effect on lightning activity are focused on cities with a population of less than 10 million, while the characteristics of lightning activity in megacities are still rarely reported. Beijing, as the capital of China, has a population of about 21 million as well as an urban area of about 16,400 km^2, which is much larger than that of previous studies [2,4,5,7,9]. In this paper, we attempt to extend the knowledge of the urban effect on lightning activity over megacities by investigating the characteristics of CG flashes in Beijing. Moreover, the comprehensive understanding of lightning activity with multi-year observation data is also the basis of effective prediction and warning of thunderstorm-related disasters in Beijing City.

2. Data and Methods

At present, the studies on lightning characteristics in Beijing are still limited. This study used an eight-year (2010–2017) CG lightning dataset from the National-Wide Lightning Detection Network operated by the State Grid Electric Power Research Institute to investigate the characteristics of lightning activity in the metropolitan area of Beijing [21]. The dataset contains information such as time, longitude, latitude, peak current, and polarity of CG strokes. The detection network combines the time-of-arrival method and the magnetic detection method to determine the geographical location of CG flashes [21]. Chen et al. [21] showed that the detection efficiency of CG flashes and CG strokes is about 94% and 60%, respectively; the arithmetic mean and the median of location errors are about 710 m and 489 m, respectively; the percentage of evaluation errors of lightning peak current is between 0.4% and 42%; the arithmetic mean and the median is about 16.3% and 19.1%, respectively. Since the detection principle, parameter setting, locating algorithm, and hardware remain unchanged, it could be used as the reference in this paper.

Previous studies indicated that this type of lightning detection network is usually contaminated by intra-cloud (IC) discharges [22–24]. Therefore, this work eliminated the misidentification of IC discharges by removing the detection results with peak current <10 kA and assuming that the rest are all CG strokes. Although the contamination level of IC discharges could still exceed this threshold, the error is almost negligible, especially for positive CG strokes that typically have high peak currents. It should be mentioned that the detection network underwent several configuration changes and performance improvements in 2009 and 2018, respectively. In order to exclude the evaluation error caused by the variation in the detection efficiency, this paper only selected the lightning detection data from 2010 to 2017.

In addition to peak current, there is another metric that has been used widely to evaluate the capacity of charge transfer by a particular lightning stroke, namely the impulse charge moment change (iCMC, defined as the product of charge transferred to ground within 2 ms after the return stroke and the original height of deposited charge in the thundercloud) [25]. Based on a three-year measurement in North America, Cummer et al. [26] provided an analytical fit for the mean iCMC as functions of peak current, by differentiating positive and negative CG strokes, as follows:

For negative CG strokes with peak current in the range of −10 to −200 kA, the analytical fit to the mean *iCMC* is

$$\overline{iCMC}^{-}\ (C{\cdot}km) = 0.53\left|I_{pk}\ (kA)\right| - 0.00086 I_{pk}^{2}\ (kA). \tag{1}$$

For positive CG strokes with peak current in the range of +40 to +200 kA, the analytical fit to the mean *iCMC* is

$$\overline{iCMC}^{-}\ (C{\cdot}km) = 0.53\left|I_{pk}\ (kA)\right| - 0.00086 I_{pk}^{2}\ (kA). \tag{2}$$

For positive CG strokes with peak current in the range of +10 to +40 kA, the analytical fit to the mean *iCMC* is

$$\overline{iCMC}^{-}\ (C{\cdot}km) = 0.53\left|I_{pk}\ (kA)\right| - 0.00086 I_{pk}^{2}\ (kA). \tag{3}$$

As shown in Figure 1a, Beijing is a city sited on the northwestern margin of the North China Plain, backed by the remaining Taihang Mountains and the Yanshan Mountains, and about 150 km from the Bohai Sea in the southeast. It is the world's most populous capital city, with over 21 million residents within an administrative area of 16,410 km^2 (http://tjj.beijing.gov.cn/EnglishSite/ accessed on 21 March 2021). Beijing is mostly surrounded by Hebei Province with the exception of neighboring Tianjin to the southeast. The topography of Beijing is generally high in the northwest and low in the southeast. The city's topography consists of two major geomorphic units: the northwestern mountains and the southeastern plains, of which 10,072 km^2 (61.4%) is mountainous and 6338 km^2 (38.6%) is plain. The average altitude of Beijing is 43.5 m above sea level, with the altitude of the plains ranging from 20 to 60 m, while the mountains are generally 1000 to 1500 m above sea level. Since the North China Plain has less topographic relief, we only plot the topographic map of mountain ranges (i.e., at altitudes >500 m above sea level). The city is about 180 km long from north to south and 160 km wide from east to west (see the inset in Figure 1a). Beijing is located in a warm-temperate semi-humid region, and its climate is a monsoon-influenced humid continental climate, with an average annual precipitation of about 600 mm in the plains. Sixty percent of its precipitation occurring in the summer months of July and August, while the air is dry during the rest of the year. The average annual temperature is about 13 °C. The monthly average temperature in January is about −3 °C, while July has an average temperature of about 27 °C. Thunderstorms in the research area are most active in summer, followed by spring and fall, while there are very few thunderstorms reported in winter. Due to the influence of the East Asian monsoon and the vast Siberian anticyclone, sandstorms blow in from the Gobi Desert across the Mongolian steppe, which is accompanied by rapid warming.

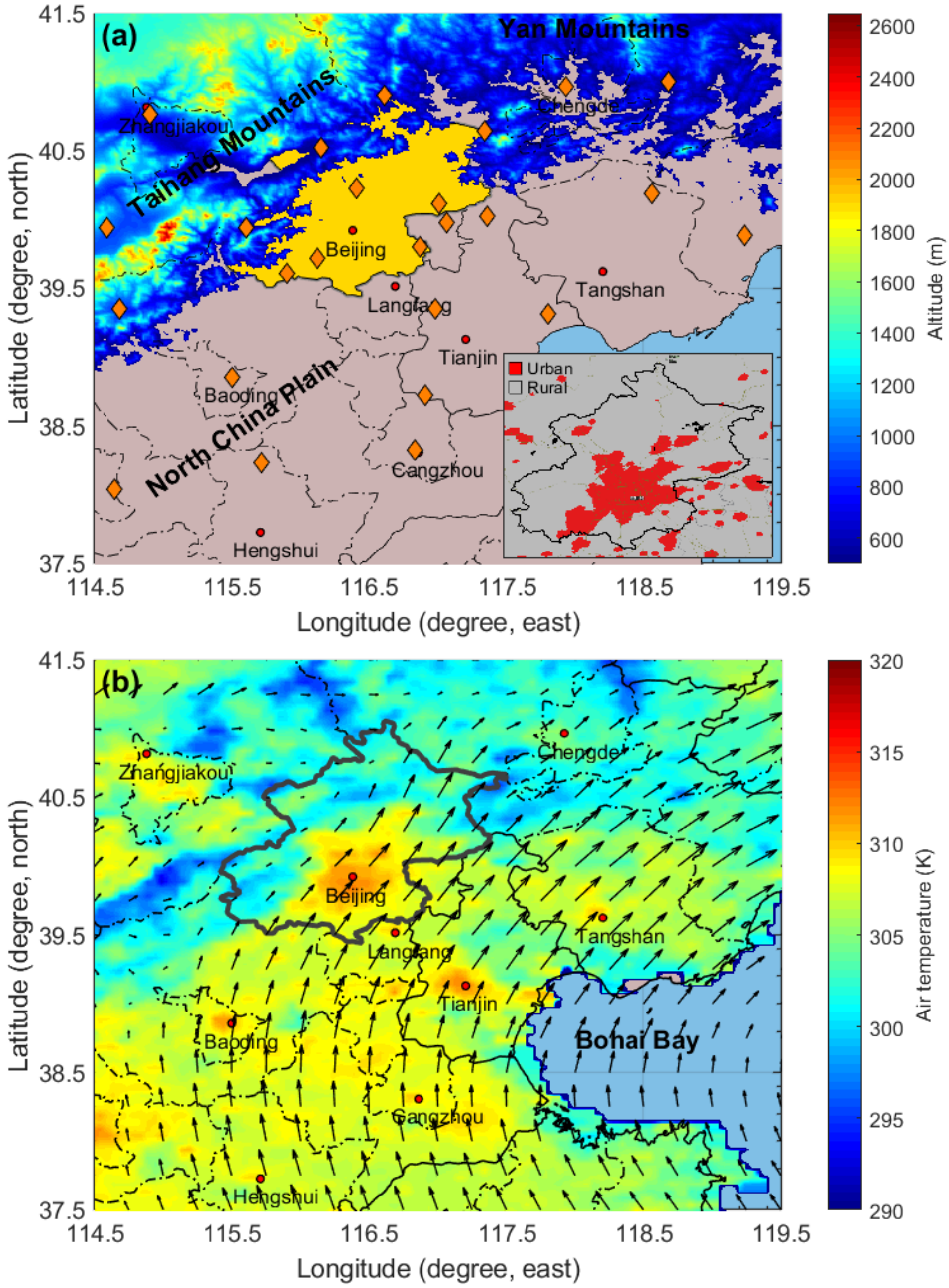

Figure 1. (**a**) Overview of the research area. Orange diamonds denote the site distribution of the National-Wide Lightning Detection Network operated by the State Grid Electric Power Research Institute. The inset shows the urban extent of Beijing provided by the United States National Aeronautics and Space Administration (NASA) (https://worldview.earthdata.nasa.gov/ accessed on 21 March 2021). (**b**) Geographical distribution of land-surface temperature and the low-altitude wind field at 925 hPa.

From the perspective of the large-scale dynamics, the season frontal systems from Mongolia and the tropical cyclones from the Western Pacific promote the development of intensive convective systems in this region. To avoid the seasonal effect, this paper only applied the average values of summer months (June–August) of land-surface temperature data (MOD11, spatial resolution: 0.05° $\times$ 0.05°) from the Moderate Resolution Imaging Spectroradiometer

(MODIS) aboard the Aqua satellite (https://modis.gsfc.nasa.gov/ accessed on 21 March 2021) as an attempt to identify the expansion of the UHI. Figure 1b shows the spatial distribution of the land-surface temperature. The results showed that the UHI effect is obvious in the downtown area of Beijing. With the increase of altitude and latitude, the land-surface temperature decreases. As the result of a correlation between lightning activity and deep convection [27–29], we also examined precipitation data (spatial resolution: $0.1° \times 0.1°$) from the Global Precipitation Measurement (GPM) (https://gpm.nasa.gov/GPM/ accessed on 21 March 2021) and balloon sounding data from the Integrated Global Radiosonde Archive (https://www.ncdc.noaa.gov/ accessed on 21 March 2021) to understand the atmospheric background status. The precipitation rate gradually increased from west to east, especially near the coastline (not shown). Precipitation averages around 570 mm annually, with close to three-quarters of that total falling from June to August. As a result of the strong convective activity in thunderstorms, in order to characterize convective weather systems with sufficient energy, we use only the available potential energy values (CAPE) of convection above the marginally unstable (>1000 J/kg). The annual mean CAPE varies from 1860 to 2820 J/kg, allowing updrafts to bring more pollutants into the cloud [28,29]. Moreover, we also analyzed the summertime wind field of the European Centre for Medium-Range Weather Forecasts (https://www.ecmwf.int/ accessed on 21 March 2021), and the results showed that the northeast of Beijing is the downwind area. The air pollution emissions of automotive vehicles and industrial activities mainly include sulfur oxides, nitrogen oxides, and particulate matter [30]. Therefore, we examined the pollutant concentration data from the Beijing Municipal Environmental Monitoring Center (http://www.bjmemc.com.cn/ accessed on 21 March 2021) to determine a possible correlation between air pollutants (including PM_{10}, $PM_{2.5}$, SO_2, and NO_2) and lightning activity. With these analyses, it is desired to more comprehensively understand the urban effect on the CG lightning activity in Beijing City.

3. Analysis and Results

The characteristics of lightning activity considerably depend on the spatial scale of thunderstorms, and thus, we classified the lightning-producing thunderstorms as local thunderstorms (that generally stay in the study area) and frontal thunderstorms (that pass through the study area). During the eight-year time period examined in this paper, a total of 632 thunderstorms were recorded in the research area, including 63 local thunderstorms and 569 frontal thunderstorms. Compared with the frontal thunderstorms, the local thunderstorms are not only less in number but also shorter in duration and smaller in scale. This indicated that the enhancement of the CG lightning density in Beijing may be mainly caused by the frontal thunderstorms associated with the mid-latitude cyclones, while the isolated thunderstorms produced by the local convection had little effect. More detailed information is shown in Table 1.

Table 1. Comparison of two types of thunderstorms.

	Number	Average Flash Number (fl)	Average Thunderstorm Lifetime (h)	Average Flash Rate (fl h^{-1})
Local convection (small scale)	63	110	4.02	82.31
Frontal systems (synoptic scale)	569	1917	12.02	139.20

The annual mean CG flash density centered in the metropolitan area of Beijing is presented in Figure 2a. Over 310,000 CG flashes were recorded in this study region from 2010 to 2017. The CG flash density ranges from less than 1 flash km^{-2} yr^{-1} in the northwestern of Beijing to over 4 flashes km^{-2} yr^{-1} in the east. The abnormally high-value area of eastern Beijing may be due to pollutants from industrial sources. Compared with the upwind area, the CG flash density of the downtown area increased by about 50%. It is noteworthy that the results of this paper are not in good agreement with those in the scientific literature [4,9]. Previous studies have shown that CG flash density is significantly enhanced both over and downwind of cities compared with other neighboring areas. However, the density-enhanced area of CG lightning was mainly concentrated in the downtown area of Beijing, and there was no obvious enhancement in the downwind area. This may be because the urbanization development of Beijing is far more than those reported cities. The UHI effect caused by the large urban sprawl has slowed down the local convection effects. Thus, it is reasonable to believe that the enhancement of urban effects on lightning activity can be weakened when the urban circulation transports pollutants over longer distances. Moreover, Tianjin is also a municipality, with a total population estimated at 15,600,000. It is one of the nine national central cities in Mainland China. It has also an obvious UHI in the urban area (Figure 1b), but the intensification of lightning activity is not significant (Figure 2a). This indicates that the UHI effect may not be the only factor in the context of high pollution.

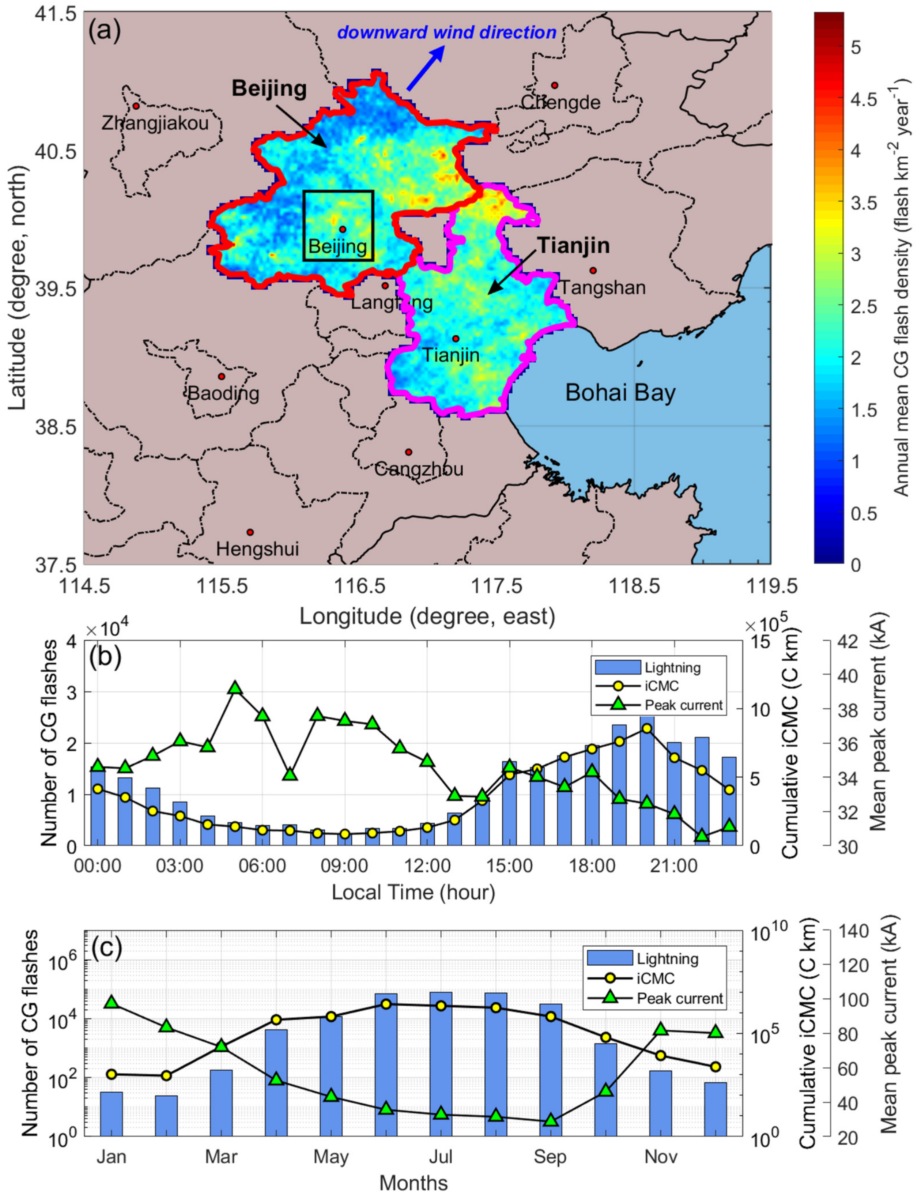

Figure 2. (**a**) Geographical distribution of the cloud-to-ground (CG) flash density. The black rectangle indicates the downtown of Beijing. (**b**,**c**) Diurnal and monthly variation of CG flash number, mean peak current, and cumulative impulse charge moment change (iCMC).

Figure 2b shows that the diurnal variation in the CG lightning number has a significant periodic tendency. Lightning activity increased from 0900 local time (LT), reached a maximum at about 2000 LT, and then slowly decreased. Previous studies have shown that the peak of lightning activity is between 1500 and 1700 LT in the continental area [31–33]. The significant increase of lightning activity in the evening is mainly because the surface temperature rises with the increase of solar radiation in the daytime. In the evening, the surface temperature and water vapor in the near-earth layer can reach high levels, which leads to convective instability in the atmosphere and further triggers thunderstorms. The reason why the peak value of lightning activity moved back in Beijing may be due to traffic pollution during the evening rush hour. The presence of high aerosol concentrations can delay the onset of precipitation and lightning activity [34]. Figure 2c shows the monthly variation of the CG flash number with a single-peak feature. About 98% of all detected CG lightning flashes occurred between May and September. The maximum and minimum of the CG flash number occurred in July and February, respectively, which also illustrates the importance of solar radiation in forcing the deep convection and forming the unstable layer. The monthly variation is similar to that reported by Holle et al. [35] who indicated that in the United States, the maximum CG flash number occurred in July, but it is different from that reported by Pinto et al. [31] who found two peaks in February and November. Pinto et al. [31] showed that the air temperature of Southeastern Brazil also has a double peak feature typical of the tropics, which confirms the tendency verified by Pinto et al. [36] of the monthly variation of the number of flashes to follow the variation of the air temperature in the tropics. North China and the Midwest of the United States are both in the middle latitudes, where only one temperature peak occurs in the summer [37,38]. Thus, differences of the temporal distribution may be related to the geographical location and climate background of different cities.

Since there is no available extremely-low-frequency (ELF, $\leq$1 kHz) data in the Beijing area to evaluate the iCMC of CG strokes [39], this paper used empirical formulas presented by Cummer et al. [26] to perform a rough evaluation (see Equations (1)–(3) in Section 2). We qualitatively estimate the charge transfer of CG strokes by adding the corresponding iCMC together. The amount of charge transfer in the thundercloud is better correlated with the lightning number, rather than the peak current, which shows that the total transferred charge is only related to the number of CG flashes. Notably, the iCMC appears to be inversely proportional to the peak current, and the charge transferring ability of lightning is stronger in winter compared to summer (see Figure 2b,c). This is likely because each discharge will "disturb" the charge distribution in the thundercloud, thus inhibiting the discharge process and causing more charges to accumulate in the charge reservoir.

Figure 3 shows the geographical distribution of the positive and negative CG flash density in the research region, with significant differences. The negative CG flashes mainly occurred in the downtown and northeastern of the city, whereas the distribution of the positive CG flashes was relatively scattered. The cloud microphysical processes that generate electric charge cannot be analyzed due to the lack of corresponding dual-polarization radar data. Existing results show that the charge reversal temperature will shift to higher temperatures when the cloud droplets contain available air pollutants [3]. Therefore, the main negative charge region can extend to the base of the cloud and cover the positive charge center below, thereby generating more negative CG flashes. For small-size graupel/ice crystals, they are better able to migrate from urban areas to suburban areas through processes of transport and dispersion of atmospheric flow. Since small-size graupel/ice crystals are positively charged between -10 and -25 °C [40,41], the positive charge region is more widely distributed and generates more positive CG lightning in suburbs. Similar lightning enhancements have been also observed in the surrounding areas of other cities, such as Baoding, Tangshan, and Cangzhou (not shown).

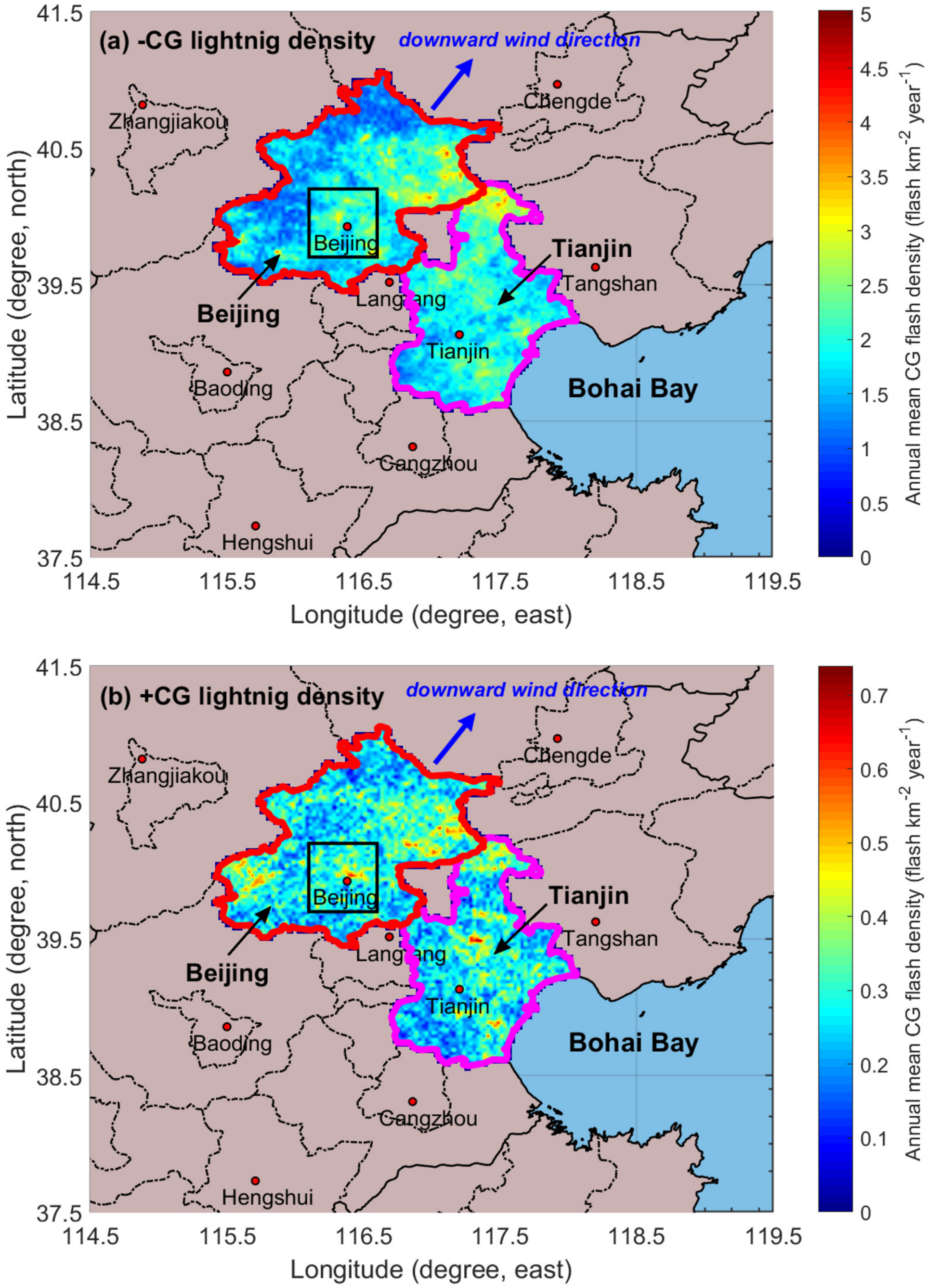

Figure 3. (**a**,**b**) Geographical distribution of the negative and positive CG lightning density. The black rectangle indicates the downtown of Beijing.

Figure 4a,b show the diurnal and monthly variations of the CG flash number with different polarities, respectively. The number of negative CG flashes (about 650,000) was much larger than that of positive CG flashes (about 100,000), and the proportion of negative CG flashes increased in summer. The diurnal and monthly variation tendency of positive and negation CG flashes is similar to that mentioned above, which will not be described here. It should be noted that the number of positive CG flashes tends to increase/decrease more slowly compared with negative CG flashes, and the mean peak current of positive CG flashes is larger than that of negative CG flashes. This paper defined the high peak current threshold as 75 kA according to the method given by Lyons et al. [42]. As illustrated in Figure 4c, the percentage of negative CG flashes with $I_{peak} \geq 75$ kA is 4.18%, while the percentage of positive CG flashes is more than 6 times (26.61%) that of the former. This may be related to the different discharge mechanisms of positive and negative CG flashes [43]. In addition, we also examined the spatial distribution of CG flashes with different peak currents. The distributions of strong CG flashes have distinct regional clustering, and they are more concentrated in downtown and industrial areas.

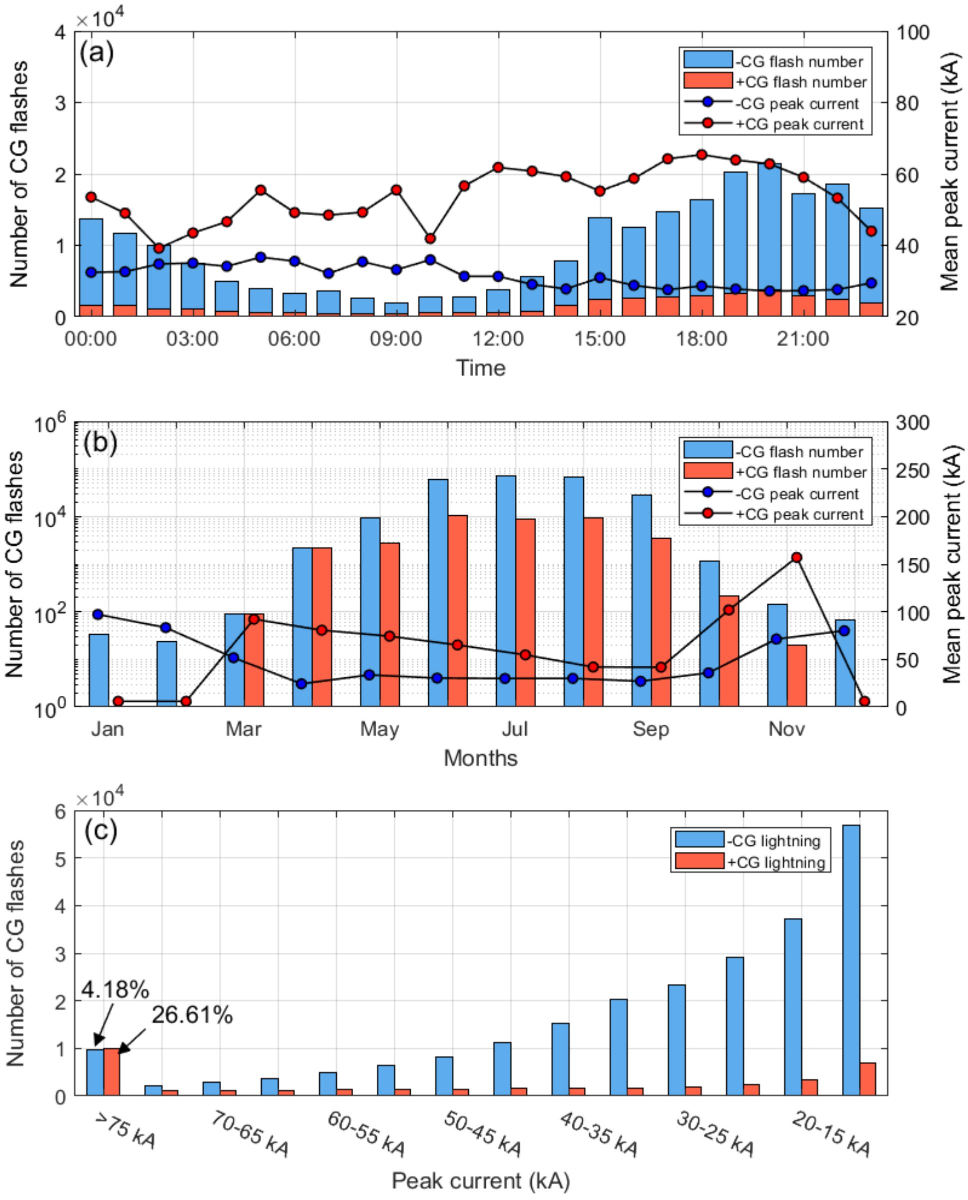

Figure 4. (**a** and **b**) Diurnal and monthly variations of CG flash number and mean peak current with different polarities. (**c**) Histogram of peak current intensity of positive and negative CG flashes.

4. Discussion

It can be seen from Figures 1b and 2a that although the UHI is an important factor in increasing lightning activity, it does not seem to be the only factor in the metropolitan area of Beijing. CG lightning activity is not only enhanced in land-surface temperature areas caused by artificial structures and the lack of vegetation, but also significantly enhanced in areas where human activity is more intense (e.g., traffic and industrial pollutant emissions. Most previous studies showed a positive correlation between pollutant concentrations and lightning activity [6,8,9,11], but a negative correlation when pollutant concentrations are high [2,10]. Although there are several different views on the details of lightning initiation [44,45], most scholars agree on the basic principle of the non-inductive charge separation process [46,47]. The augment of pollutants could affect the cloud electrification by altering the concentration, phase, size, and surface property of graupel/ice crystals in the mixed-phase region (from 0 to −40 °C), resulting in the generation of more CG lightning [41,48].

To ascertain the possible effect of anthropogenic pollutants, we examined the correlation between the CG flash number of 222 thunderstorms passing through the downtown and average concentrations of corresponding pollutants (i.e., SO_2, NO_2, $PM_{2.5}$, and PM_{10}). However, no significant correlation was found in scatter plots (Figure 5b–e). We also examined the temporal relation of the CG flash number and pollutant concentrations in the vicinity of air pollution monitoring stations (red rectangle in Figure 5a).

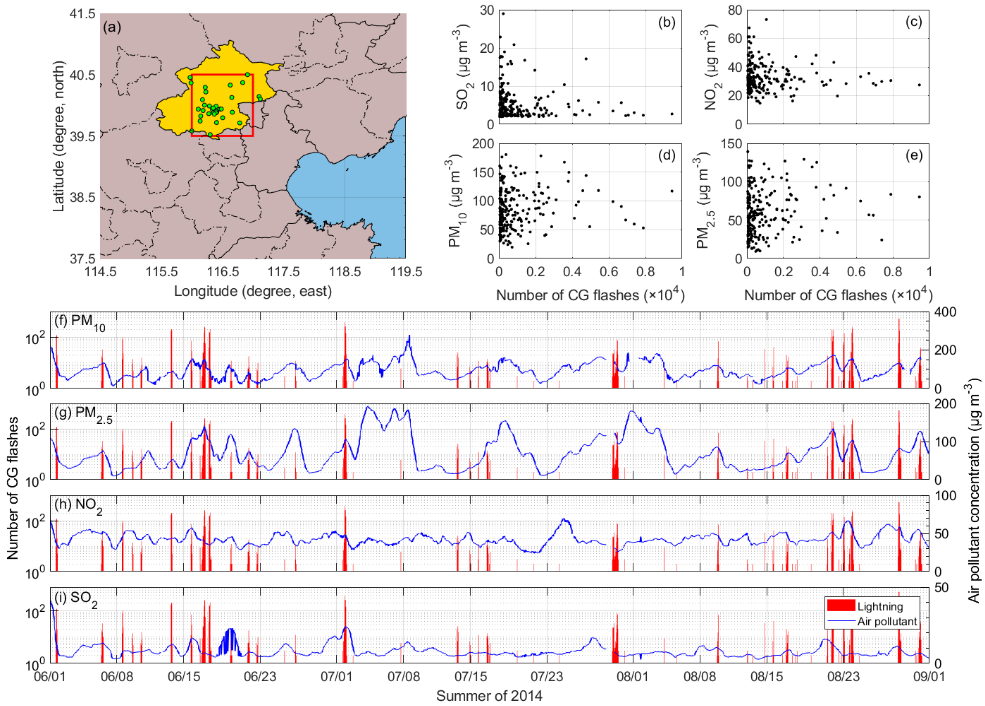

Figure 5. (**a**) Spatial distribution of the annual mean ultraviolet aerosol index and air pollution monitoring stations. The red rectangle represents the statistical area of the CG flash number near the monitoring station. (**b**–**e**) Scatter plots of CG flash number and mean concentrations of SO_2, NO_2, $PM_{2.5}$, and PM_{10}. (**f**–**i**) Temporal distribution of pollutant concentrations and CG flash number.

This paper takes the summer season of 2014 as an example. The peak value of the CG flash number usually corresponds to the peak value of pollutant concentrations in a period of time, and it has a slight delay, especially for particulate matter (Figure 5f–i). However, the corresponding relationship is not absolute, and the occurrence of lightning sometimes does not correlate with the concentration of pollutants. This is because the pollutant concentration varies with different meteorological conditions, so it is difficult to quantify the contribution of air pollution to the enhancement of overall lightning activity. Soriano and de Pablo [4] have also indicated that PM_{10} is a non-influential parameter for enhancing urban lightning activity. In addition, the aerosol could reduce the electrical activity by absorbing solar radiation [18,49,50], which also suppresses the deep convection and the relative humidity [7,51]. In summary, the lightning activity is influenced by a variety of factors (e.g., urban heat island circulation, frictional lift, aerosol increase, cloud water content, etc.), and further research is needed in the future work to clarify the physical mechanisms that lead to lightning enhancement.

Since the air pollution monitoring stations are mostly deployed in urban areas and only a few are installed in agricultural and industrial areas (see Figure 5a), they can only represent the situation in a limited area. This is very mismatched with the wide spatial distribution of lightning activity. The suburbs of Beijing have dense infrastructures such as refineries, chemical facilities, steelworks, and power plants, but the overall population is low and the urban development is slight. Thus, we also examined the ultraviolet (270–380 nm) aerosol index (UVAI) data (spatial resolution: 13 km × 12 km) from the Ozone Monitoring Instrument (OMI) aboard the Aura satellite (http://projects.knmi.nl/omi/ accessed on 21 March 2021) to verify the aerosol optical depth in non-urban areas [52,53]. However, unfortunately, the scanning range of the satellite orbit is limited, so the relevant data corresponding to the study area cannot be obtained. We examined the correlation between the concentration of pollutants and the lightning activity, and the results showed there was a good spatial correspondence between the high lightning density and the high aerosol concentration in Baoding (not shown). Industrial pollution may play a greater role than domestic pollution. As it is not relevant to the presentation of this paper, we will make an in-depth analysis of the relevant content in the follow-up work.

5. Conclusions

Even though the local enhancement of lightning activity in the urban areas has been studied extensively, the urban effect of megacities is still lacking. In this work, an eight-year CG lightning dataset was investigated to study the long-term behavior of lightning activity in the metropolitan area of Beijing. The dataset was analyzed from both spatial and temporal perspectives, and the paper also examined the correlation between lightning activity and other parameters such as land-surface temperature and pollutants. The high CG lightning density area was mainly concentrated in the downtown of Beijing, but there was no remarkable enhancement in the downwind area. The CG flash density in the downtown was about 50% higher than that of the upwind area. About 98% of CG flashes mainly occurred from May to September and the enhancement of CG diurnal variation was most pronounced from 1900 to 2100 LT. Negative CG lightning mainly occurred in the downtown and industrial area, while the distribution of the positive CG flashes was relatively scattered. The percentage of positive CG lightning with $I_{peak} \geq 75$ kA is more than six times that of the negative CG flashes. By comparing the spatial relationship between the UHI and the CG lightning density in surrounding cities and industrial areas, the enhancement of lightning activity is influenced by multiple factors. Therefore, longer periods and more precise observational studies from different regions of the globe are required.

Author Contributions: Y.W. (Yongping Wang) was responsible for data curation and management, and wrote the whole of this paper. Y.W. (Yu Wang) was a supervisor of this research project and provided funding, data sources, methodology of data curation. G.L. was a principal investigator and a supervisor of this research project, and provided funding. T.S. and C.P. conducted literature research on urban lightning activity. M.M., revised the manuscript. B.Z. and D.L. provided meteorological data. All authors have read and agreed to the published version of the manuscript.

Funding: This research was funded by "Natural Science Foundation of China (52007037)", "Science and Technology Program of State Grid Corporation of China (524625200017)", "National Key R&D Program of China (2017YFC1501501)", and "Natural Science Foundation of China (41875006, U1938115)".

Data Availability Statement: The data examined in this paper are available at https://doi.org/10.5281/zenodo.4430092 (accessed on 21 March 2021).

Acknowledgments: We acknowledge the Goddard Earth Sciences Data and Information Services Center (https://disc.gsfc.nasa.gov/ accessed on 21 March 2021) and the European Centre for Medium-Range Weather Forecasts (https://www.ecmwf.int/ accessed on 21 March 2021) for the dissemination of data as well as sounding data from the Integrated Global Radiosonde Archive (https://www.ncdc.noaa.gov/ accessed on 21 March 2021).

Conflicts of Interest: The authors declare no conflict of interest.

References

1. Huff, F.A.; Changnon, S.A. precipitation modification by major urban areas. *Bull. Am. Meteorol. Soc.* **1973**, *54*, 1220–1233. [CrossRef]
2. Westcott, N.E. Summertime Cloud-to-Ground Lightning Activity around Major Midwestern Urban Areas. *J. Appl. Meteorol.* **1995**, *34*, 1633–1642. [CrossRef]

3. Steiger, S.M.; Huffines, G.; Orville, R.E. Cloud-to-ground lightning characteristics over Houston, Texas: 1989–2000. *J. Geophys. Res. Space Phys.* **2002**, *107*. [CrossRef]
4. Soriano, L.R.; de Pablo, F. Effect of small urban areas in central Spain on the enhancement of cloud-to-ground lightning activity. *Atmos. Environ.* **2002**, *36*, 2809–2816. [CrossRef]
5. Orville, R.E.; Huffines, G.; Nielsen-Gammon, J.; Zhang, R.; Ely, B.; Steiger, S.; Phillips, S.; Allen, S.; Read, W. Enhancement of cloud-to-ground lightning over Houston, Texas. *Geophys. Res. Lett.* **2001**, *28*, 2597–2600. [CrossRef]
6. Naccarato, K.P.; Pinto, O., Jr.; Pinto, I.R.C.A. Evidence of thermal and aerosol effects on the cloud-to-ground lightning density and polarity over large urban areas of Southeastern Brazil. *Geophys. Res. Lett.* **2003**, *30*. [CrossRef]
7. Lal, D.; Pawar, S. Effect of urbanization on lightning over four metropolitan cities of India. *Atmos. Environ.* **2011**, *45*, 191–196. [CrossRef]
8. Kar, S.; Liou, Y.-A.; Ha, K.-J. Aerosol effects on the enhancement of cloud-to-ground lightning over major urban areas of South Korea. *Atmos. Res.* **2009**, *92*, 80–87. [CrossRef]
9. Kar, S.; Liou, Y. Enhancement of cloud-to-ground lightning activity over Taipei, Taiwan in relation to urbanization. *Atmos. Res.* **2014**, *147–148*, 111–120. [CrossRef]
10. Farias, W.; Pinto, O.; Pinto, I.; Naccarato, K. The influence of urban effect on lightning activity: Evidence of weekly cycle. *Atmos. Res.* **2014**, *135–136*, 370–373. [CrossRef]
11. Farias, W.; Pinto, O.; Naccarato, K.; Pinto, I. Anomalous lightning activity over the Metropolitan Region of São Paulo due to urban effects. *Atmos. Res.* **2009**, *91*, 485–490. [CrossRef]
12. Bourscheidt, V.; Pinto, O., Jr.; Naccarato, K.P. The effects of Sao Paulo urban heat island on lightning activity: Decadal analysis (1999–2009). *J. Geophys. Res.* **2016**, *121*, 4429–4442. [CrossRef]
13. Rozoff, C.M.; Cotton, W.R.; Adegoke, J.O. Simulation of St. Louis, Missouri, Land Use Impacts on Thunderstorms. *J. Appl. Meteorol.* **2003**, *42*, 716–738. [CrossRef]
14. Han, J.-Y.; Baik, J.-J. A Theoretical and Numerical Study of Urban Heat Island–Induced Circulation and Convection. *J. Atmos. Sci.* **2008**, *65*, 1859–1877. [CrossRef]
15. van den Heever, S.C.; William, R.C. Urban Aerosol Impacts on Downwind Convective Storms. *J. Appl. Meteorol. Clim.* **2007**, *46*, 828–850. [CrossRef]
16. Ntelekos, A.A.; Smith, J.A.; Donner, L.; Fast, J.D.; Gustafson, W.I., Jr.; Chapman, E.G.; Krajewski, W.F. The effects of aerosols on intense convective precipitation in the northeastern United States. *Q. J. R. Meteorol. Soc.* **2009**, *135*, 1367–1391. [CrossRef]
17. Bréon, F.-M.; Tanré, D.; Generoso, S. Aerosol Effect on Cloud Droplet Size Monitored from Satellite. *Science* **2002**, *295*, 834–838. [CrossRef]
18. Altaratz, O.; Koren, I.; Yair, Y.; Price, C. Lightning response to smoke from Amazonian fires. *Geophys. Res. Lett.* **2010**, *37*. [CrossRef]
19. Wang, Q.; Li, Z.; Guo, J.; Zhao, C.; Cribb, M. The climate impact of aerosols on the lightning flash rate: Is it detectable from long-term measurements? *Atmos. Chem. Phys.* **2018**, *18*, 12797–12816. [CrossRef]
20. Tan, Y.B.; Peng, L.; Shi, Z.; Chen, H.R. Lightning flash density in relation to aerosol over Nanjing (China). *Atmos. Res.* **2016**, *174–175*, 1–8.
21. Chen, L.; Zhang, Y.; Lu, W.; Zheng, D.; Zhang, Y.; Chen, S.; Huang, Z. Performance Evaluation for a Lightning Loca-tion System Based on Observations of Artificially Triggered Lightning and Natural Lightning Flashes. *J. Atmos. Ocean. Technol.* **2012**, *29*, 1835–1844. [CrossRef]
22. Cummins, K.L.; Murphy, M.J.; Bardo, E.A.; Hiscox, W.L.; Pyle, R.B.; Pifer, A.E. A Combined TOA/MDF Technology Upgrade of the U.S. National Lightning Detection Network. *J. Geophys. Res. Space Phys.* **1998**, *103*, 9035–9044. [CrossRef]
23. Orville, R.E.; Huffines, G.R.; Burrows, W.R.; Holle, R.L.; Cummins, K.L. The North American Lightning Detection Network (NALDN)—First Results: 1998–2000. *Mon. Weather Rev.* **2002**, *130*, 2098–2109. [CrossRef]
24. Schulz, W.; Cummins, K.; Diendorfer, G.; Dorninger, M. Cloud-to-ground lightning in Austria: A 10-year study using data from a lightning location system. *J. Geophys. Res. Space Phys.* **2005**, *110*. [CrossRef]
25. Cummer, S.A.; Lyons, W.A. Implications of lightning charge moment changes for sprite initiation. *J. Geophys. Res. Space Phys.* **2005**, *110*. [CrossRef]
26. Cummer, S.A.; Lyons, W.A.; Stanley, M.A. Three years of lightning impulse charge moment change measurements in the United States. *J. Geophys. Res. Atmos.* **2013**, *118*, 5176–5189. [CrossRef]
27. Dai, J.; Wang, Y.; Chen, L.; Tao, L.; Gu, J.; Wang, J.; Xu, X.; Lin, H.; Gu, Y. A comparison of lightning activity and convective indices over some monsoon-prone areas of China. *Atmos. Res.* **2009**, *91*, 438–452. [CrossRef]
28. Siingh, D.S.; Kumar, P.R.; Kulkarni, M.; Singh, R.; Singh, A. Lightning, convective rain and solar activity—Over the South/Southeast Asia. *Atmos. Res.* **2013**, *120–121*, 99–111. [CrossRef]
29. Siingh, D.; Buchunde, P.; Singh, R.; Nath, A.; Kumar, S.; Ghodpage, R. Lightning and convective rain study in different parts of India. *Atmos. Res.* **2014**, *137*, 35–48. [CrossRef]
30. Zhang, R.; Wang, G.; Guo, S.; Zamora, M.L.; Ying, Q.; Lin, Y.; Wang, W.; Hu, M.; Wang, Y. Formation of Urban Fine Particulate Matter. *Chem. Rev.* **2015**, *115*, 3803–3855. [CrossRef]
31. Pinto, O.; Pinto, I.R.C.; Diniz, J.H.; Filho, A.C.; Cherchiglia, L.C.; Carvalho, A.M. A seven-year study about the negative cloud-to-ground lightning flash characteristics in Southeastern Brazil. *J. Atmos. Solar Terr. Phys.* **2003**, *65*, 739–748. [CrossRef]

32. Holle, R.L. Diurnal Variations of NLDN-Reported Cloud-to-Ground Lightning in the United States. *Mon. Weather Rev.* **2014**, *142*, 1037–1052. [CrossRef]
33. Chronis, T.G.; Cummins, K.L.; Said, R.K.; Koshak, W.J.; McCaul, E.W.; Williams, E.R.; Stano, G.T.; Grant, M.R. Climatological diurnal variation of negative CG lightning peak current over the continental United States. *J. Geophys. Res. Atmos.* **2015**, *120*, 582–589. [CrossRef]
34. Guo, J.; Deng, M.; Lee, S.S.; Wang, F.; Li, Z.; Zhai, P.; Liu, H.; Lv, W.; Yao, W.; Li, X. Delaying precipitation and lightning by air pollution over the Pearl River Delta. Part I: Observational analyses. *J. Geophys. Res. Atmos.* **2016**, *121*, 6472–6488. [CrossRef]
35. Holle, R.L.; Cummins, K.L.; Brooks, W.A. Seasonal, Monthly, and Weekly Distributions of NLDN and GLD360 Cloud-to-Ground Lightning. *Mon. Weather Rev.* **2016**, *144*, 2855–2870. [CrossRef]
36. Pinto, I.R.C.A.; Pinto, O.; Rocha, R.M.L.; Diniz, J.H.; Carvalho, A.M.; Filho, A.C. Cloud-to-ground lightning in southeastern Brazil in 1993: 2. Time variations and flash characteristics. *J. Geophys. Res. Space Phys.* **1999**, *104*, 31381–31387. [CrossRef]
37. Orville, R.E.; Silver, A.C. Lighting Ground Flash Density in the Contiguous United States: 1992–95. *Mon. Weather Rev.* **1997**, *125*, 631–638. [CrossRef]
38. Orville, R.E.; Huffines, G.R. Lightning Ground Flash Measurements over the Contiguous United States: 1995–97. *Mon. Weather Rev.* **1999**, *127*, 2693–2703. [CrossRef]
39. Cummer, S.A.; Inan, U.S. Modeling ELF radio atmospheric propagation and extracting lightning currents from ELF obser-vations. *Radio Sci.* **2000**, *35*, 385–394. [CrossRef]
40. Avila, E.E.; Pereyra, R.G.; Varela, G.G.A.; Caranti, G.M. The effect of the cloud-droplet spectrum on electrical-charge transfer during individual ice-ice collisions. *Q. J. R. Meteorol. Soc.* **1999**, *125*, 1669–1679. [CrossRef]
41. Zhao, P.; Yin, Y.; Xiao, H. The effects of aerosol on development of thunderstorm electrification: A numerical study. *Atmos. Res.* **2015**, *153*, 376–391. [CrossRef]
42. Lyons, W.A.; Uliasz, M.; Nelson, T.E. Large Peak Current Cloud-to-Ground Lightning Flashes during the Summer Months in the Contiguous United States. *Mon. Weather Rev.* **1998**, *126*, 2217–2233. [CrossRef]
43. Rakov, V.A.; Uman, M.A. *Lightning: Physics and Effects*; Cambridge University Press: Cambridge, UK, 2003.
44. Dwyer, J.R. The initiation of lightning by runaway air breakdown. *Geophys. Res. Lett.* **2005**, *32*. [CrossRef]
45. Gurevich, A.V.; Zybin, K.P. Runaway breakdown and the mysteries of lightning. *Phys. Today* **2005**, *58*, 37–43. [CrossRef]
46. Takahashi, T. Riming Electrification as a Charge Generation Mechanism in Thunderstorms. *J. Atmos. Sci.* **1978**, *35*, 1536–1548. [CrossRef]
47. Williams, E.R.; Zhang, R.; Rydock, J. Mixed-Phase Microphysics and Cloud Electrification. *J. Atmos. Sci.* **1991**, *48*, 2195–2203. [CrossRef]
48. Rosenfeld, D.; Lensky, I.M. Satellite–Based Insights into Precipitation Formation Processes in Continental and Maritime Convective Clouds. *Bull. Am. Meteorol. Soc.* **1998**, *79*, 2457–2476. [CrossRef]
49. Koren, I.; Martins, J.V.; Remer, L.A.; Afargan, H. Smoke Invigoration Versus Inhibition of Clouds over the Amazon. *Science* **2008**, *321*, 946–949. [CrossRef]
50. Rosenfeld, D. Suppression of Rain and Snow by Urban and Industrial Air Pollution. *Science* **2000**, *287*, 1793–1796. [CrossRef]
51. Rosenfeld, D.; Lohmann, U.; Raga, G.B.; O'Dowd, C.D.; Kulmala, M.; Fuzzi, S.; Reissell, A.; Andreae, M.O. Flood or Drought: How Do Aerosols Affect Precipitation? *Science* **2008**, *321*, 1309–1313. [CrossRef]
52. Torres, O.; Bhartia, P.K.; Herman, J.R.; Ahmad, Z.; Gleason, J. Derivation of aerosol properties from satellite meas-urements of backscattered ultraviolet radiation: Theoretical basis. *J. Geophys. Res.* **1998**, *103*, 17099–17110. [CrossRef]
53. Torres, O.; Bhartia, P.K.; Herman, J.R.; Sinyuk, A.; Ginoux, P.; Holben, B. A Long-Term Record of Aerosol Optical Depth from TOMS Observations and Comparison to AERONET Measurements. *J. Atmos. Sci.* **2002**, *59*, 398–413. [CrossRef]